Research Article | Vol. 28, No. 5 / 2 March 2020 / Optics Express 6937
Optics EXPRESS

Broad bandwidth dual-wavelength fiber laser simultaneously delivering stretched pulse and dissipative soliton

XINXIN JIN,[1] MENG ZHANG,[1,*] GUOHUA HU,[2,3] QING WU,[1] ZHENG ZHENG,[1,4] AND TAWFIQUE HASAN[2]

[1] School of Electronic and Information Engineering, Beihang University, Beijing, 100191, China
[2] Cambridge Graphene Centre, University of Cambridge, Cambridge, CB3 0FA, UK
[3] Department of Electronic Engineering, The Chinese University of Hong Kong, Hong Kong, China
[4] Beijing Advanced Innovation Center for Big Data-Based Precision Medicine, Beihang University, Beijing 100083, China
[*] mengzhang10@buaa.edu.cn

Abstract: We numerically and experimentally demonstrate the generation of broad bandwidth mode-locked dual-wavelength pulses with diverse-pattern from a dispersion managed erbium-doped (Er-doped) fiber laser. The two-peak gain profile of the Er-doped fiber is shown to have advantages in achieving broadband dual-wavelength pulses compared to a comb filter in our cavity. Our obtained bandwidths of 24 nm and 11.5 nm represent the broadest achieved in an Er-doped dual-wavelength fiber laser to date. In addition, the weak third-order dispersion (TOD) of the fibers facilitates two dispersion-pattern pulses (one stretched pulse and one dissipative soliton) generated in the near zero dispersion regime. Our results provide a convenient, effective way to obtain such sources for potential applications, such as in dual-comb metrology and multicolor pulses in nonlinear microscopy.

1. Introduction

Laser sources that simultaneously generate multi-wavelength pulses have attracted extensive attention due to their potential applications that single-wavelength lasers are not sufficient [1–4]. In particular, low-cost and compact erbium-doped (Er-doped) fiber lasers simultaneously producing asynchronous dual-wavelength ultrashort pulses have been extensively deployed for applications in pump-probe measurement and broadband optical and terahertz spectroscopy [5–8]. To date, several schemes have been proposed to produce dual-wavelength pulses. One effective method is to add an additional route in a laser cavity that allows dual-wavelength pulses circulating along two-branches or dual-cavity-loop separately [9–12]. By designing different physical parameters (e.g. fiber length, dispersion and nonlinearity) of the two routes, two asynchronous pulses with significantly different properties could be achieved. However, the generated pulses from the two routes have reduced mutual coherence as they propagate through different physical paths. Another effective method to obtain dual-wavelength pulses is to introduce comb filtering effect into the cavity. As the dual-wavelength pulses propagate through the same physical path, this method endows the dual-wavelength pulses with passively maintained mutual coherence due to common mode environmental noise rejection [13,14]. The spectral filtering effect can be introduced by the periodic wavelength-dependence-reflectivity of a saturable absorber (SA) [15], multimode interference effect [16,17], or birefringence-induced comb filtering effect [18–21]. These filters have a good flexibility as their filter period, center wavelength and modulation depth can be conveniently tuned by changing corresponding parameters, such as device length and fiber birefringence [16–21]. Previous demonstrations have shown that large modulation depth (generally > 3 dB) of the filter should be satisfied to isolate adjacent gain channels. However,

#385142 https://doi.org/10.1364/OE.385142
Journal © 2020 Received 12 Dec 2019; revised 20 Jan 2020; accepted 28 Jan 2020; published 24 Feb 2020

Optics EXPRESS

while the filter period is fixed, large modulation depth leads to a narrower filter bandwidth and thus, narrower pulse spectral bandwidth [22]. This is especially true for Er-doped fiber lasers as erbium-doped fiber (EDF) generally has a much smaller gain bandwidth compared to that of thulium-doped fiber (TDF) and Ytterbium-doped fiber (YDF). Achieving broad bandwidth dual-wavelength pulses from Er-doped fiber lasers is therefore very challenging. Indeed, the reported full width at half maximum (FWHM) bandwidth of dual-wavelength Er-doped fiber lasers to date is limited to ~10 nm [23]. Alternatively, EDF could exhibit saddle-like gain profile with two gain peaks under certain pump and signal conditions, providing another viable solution for dual-wavelength operation [2,24–26]. However, the potential of the two-peak gain profile of EDF for large bandwidth dual-wavelength pulses generation is yet to be investigated.

On the other hand, there has been growing interest in exploring dual-wavelength mode-locked fiber lasers producing diverse patterns [27–32]. In terms of simultaneous generation of different dispersion pattern solitons, the previous reports need either complicated cavity design [9] or specific long fibers with strong third-order dispersion (TOD) [32]. By introducing 10 m dispersion compensation fiber (DCF) with TOD of 1.67 ps^3/km, Wang *et al.* demonstrated the coexistence of dissipative soliton (DS) and stretched pulse (SP) in a dual-wavelength mode-locked thulium-doped (Tm-doped) fiber laser [32]. The longer DCF used in their cavity could lead to unstable stationary pulse regime because of the long laser cavity and high nonlinearity coefficient of the DCF. We propose that the coexistence of these two dispersion pattern pulses can also be achieved without the use of long DCF with strong TOD.

Here, we propose a dual-wavelength mode-locked Er-doped fiber laser operating at near zero dispersion that only consists of single-mode fibers with a weak TOD (0.3 ps^3/km). Both numerical and experimental results confirm its capability of delivering DS and SP simultaneously. By taking advantage of the two gain peaks of EDF without introducing any spectral filtering effects, both the DS and SP soliton achieve the widest bandwidth compared to any previously reported Er-doped dual-wavelength fiber lasers. The proposed simple, compact laser is of significant importance for diverse-pattern dual-wavelength pulses generation, and for applications requiring wide bandwidth asynchronous dual-wavelength laser sources.

2. Laser setup

The schematic of the dual-wavelength Er-doped fiber laser is shown in Fig. 1. A piece of 3.5 m EDF (YOFC-EDF1022) with a group-velocity dispersion (GVD) of 20 ps^2/km at 1.55 μm is co-pumped by a 980 nm pump laser diode through a 1 m 980/1550 nm wavelength division multiplexer (WDM, where its pigtail consists of HI1060 fiber with a GVD of -7 ps^2/km at 1.55 μm). In addition to the EDF and WDM, all the pigtails of the rest components in the cavity are made of single mode fiber (SMF) with a GVD of -22 ps^2/km at 1.55 μm, including a 20% output coupler, an inline polarization-independent optical isolator and two polarization controllers (PCs) to balance the gain profile of the EDF by controlling the loss of the cavity. The inkjet-printed black phosphorus(BP), passivated with Parylene C for environmental stability, that has been successfully demonstrated as a broadband passive switch for ultrafast lasers [33,34], is

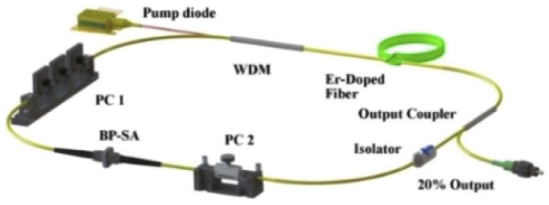

Fig. 1. Schematic of the dual-wavelength Er-doped fiber laser.

Optics EXPRESS

sandwiched between two fiber connectors as SA. The total cavity length is 7.1 m. The net cavity dispersion is calculated as ~ 0.0058 ps^2 at 1.55 μm, indicating the laser operates at near zero dispersion. It is important to note that no polarization maintaining fiber (PMF) is used.

3. Numerical simulation

To explore the formation mechanism of the dual-wavelength pulses from the Er-doped laser setup, we perform numerical simulations based on the nonlinear Schrödinger equation (NLSE),

$$\frac{\partial U}{\partial Z} = -i\frac{\beta_2}{2}\frac{\partial^2 U}{\partial t^2} + \frac{\beta_3}{6}\frac{\partial^3 U}{\partial t^3} + i\gamma|U|^2U + \frac{g}{2}U + \frac{g}{2\Omega_g{}^2}\frac{\partial^2 U}{\partial t^2}, \tag{1}$$

where U is the envelope of the field, β_2 is the GVD parameter, β_3 is the TOD parameter, Z is the propagation distance, t is the time, γ is the nonlinear parameter, and Ω_g is the gain bandwidth. The laser gain g is given by $g = G\exp(-P_{ave}/P_{sat})$, where G is the small signal gain coefficient, P_{sat} is the gain saturation power determined by the pump power, and P_{ave} is the average power. The transmittance of BP-SA is expressed by $T = 1\text{-}\alpha_{ns}\text{-}\alpha_0/(1+I/I_{sat})$, where α_0 is modulation depth, α_{ns} is non-saturation absorption, and I_{sat} is the saturation intensity. A main modification in the gain spectrum is used to simulate the dual-wavelength mode-locking. The normalized gain spectrum is modeled as a saddle-like profile [2,35], where the two peaks (i.e., 1530 and 1556 nm) correspond to high transmission while the valley corresponds to a low transmission, indicated by black dotted line, shown in Fig. 2. The TOD parameter of all the fibers is set as 0.3 ps^3/km. The detailed parameters used in the numerical model are listed in Table 1.

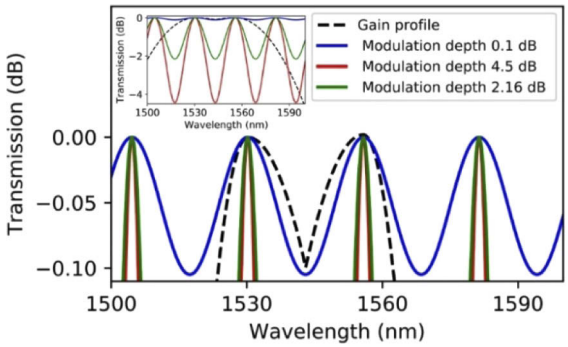

Fig. 2. Gain profile and intra-cavity comb filter transmission curves with different modulation depths. Inset shows the gain profile and transmission curves in larger Y-axis.

Table 1. Fiber parameters of the numerical simulations

EDF	SMF	HI1060	BP-SA
$\beta_2 = 20$ ps^2/km	$\beta_2 = -22$ ps^2/km	$\beta_2 = -7$ ps^2/km	$\alpha_0 = 10.03\%$
$\beta_3 = 0.3$ ps^3/km	$\beta_3 = 0.3$ ps^3/km	$\beta_3 = 0.3$ ps^3/km	$\alpha_{ns} = 9.97\%$
$\gamma = 2.3$ $W^{-1}km^{-1}$	$\gamma = 1.1$ $W^{-1}km^{-1}$	$\gamma = 1.5$ $W^{-1}km^{-1}$	$I_{sat} = 13.3$ W
$L = 3.5$ m; $G = 0.63$;	$L = 2.6$ m	$L = 1$ m	

In the simulation, an initial weak pulse could evolve to a stable dual-wavelength mode locking state when $P_{sat} = 4.05$ mW. Figures 3(a) and 3(b) shows the evolution of the spectrum and the waveform as a function of the roundtrips, respectively. The saddle-like gain spectrum provides two gain peaks, corresponding to two gain channels. The spectrum of the initial weak pulse splits into two that located on the two gain channels after several roundtrips. The isolation of

Optics EXPRESS

the two spectra is then enhanced each time the pulses cycling through the saddle-like gain fiber. Finally, the gain competition of the two spectra (corresponding to two pulses) reaches equilibrium after ~500 roundtrips and the stable dual-wavelength mode locking is obtained. The evolution traces of the two pulses in Fig. 3(b) have different slope, indicating that they are asynchronous dual-wavelength pulses. While the dual-wavelength spectrum centered at 1530 nm shows steep spectral edges and flat spectral top with a FWHM of 11 nm, the spectrum centered at 1556 nm has a broad spectral FWHM of 22 nm [Fig. 3(c)]. The time domain shows two pulses with different peak power and pulse width [Fig. 3(d)]. To further confirm the dispersion feature of the two pulses, the variation of the pulse duration and frequency chirp of the asynchronous pulses in one round trip are also investigated. We characterize the frequency chirp by calculating the slope of chirp at the center of the pulses. Starting from the EDF, the pulse with lower peak power breathes once in one roundtrip and is always up-chirped through the whole cavity [Fig. 3(e)]. The high peak power pulse breathes twice with alternating frequency chirp in the cavity [Fig. 3(f)]. The simulation results agree well with the typical features of a DS and an SP [32,36], respectively. Therefore, the coexistence of these two dispersion pattern pulses can be achieved in laser cavity that only consists of fibers with a weak TOD.

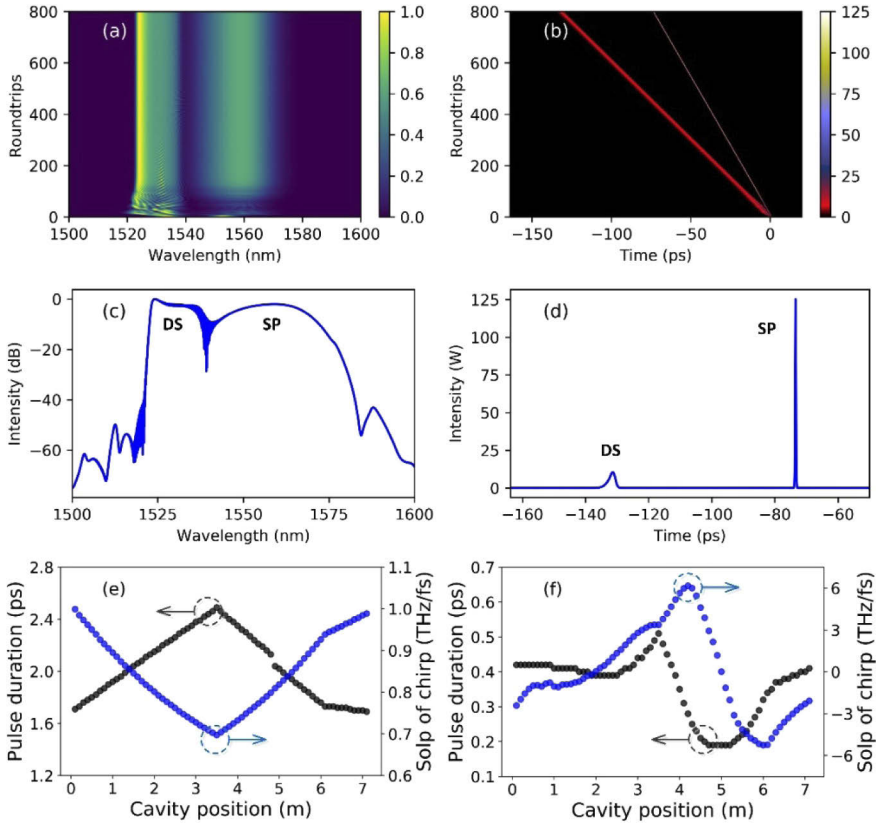

Fig. 3. Simulated results of broad bandwidth dual-wavelength pulses with saddle-like gain profile: evolution of (a) normalized spectrum in linear scale and (b) waveform as a function of roundtrips; (c) normalized spectrum and (d) waveform at roundtrip of 800 with spectral bandwidth of 11 nm and 22 nm, respectively; the variation of pulse duration and slope of chirp of (e) DS and (f) SP along the laser cavity.

To demonstrate that the saddle-like gain profile is indeed better than a comb filter in terms of facilitating broad bandwidth dual-wavelength pulses, we substitute a comb filter in the laser cavity

Optics EXPRESS

for the saddle-like gain profile while keeping the other parameters of the cavity unchanged. The comb filter period of 26 nm in our simulations is consistent with the separation of the two gain peaks of the saddle-like profile. The modulation depth of the comb filter is firstly set as 0.1 dB, which is comparable to the peak-dip difference of the saddle-like gain profile (labeled using the blue line in Fig. 2), leading to a single-wavelength mode-locking operation. A typical result of the simulation at the P_{sat} of 1.45 mW is shown by the single-wavelength spectrum [Fig. 4(a)] and single pulse in the time domain [Fig. 4(b)]. The results are attributed to the low modulation depth of the comb filter. Unlike saddle-like gain profile of EDF, which can promote the formation of dual-wavelength along the whole length of gain fiber, the comb filtering effect only exists at one point in the cavity (e.g. polarizer) and thus the effect is weak at low modulation depth. We then change the comb filter modulation depth to 4.5 dB, as shown using the red line in Fig. 2. Under this condition, we could obtain a dual-wavelength mode-locking at the P_{sat} of 0.87 mW with FWHM of 8 nm and 6 nm, respectively. The spectral bandwidth increases when increasing P_{sat}.

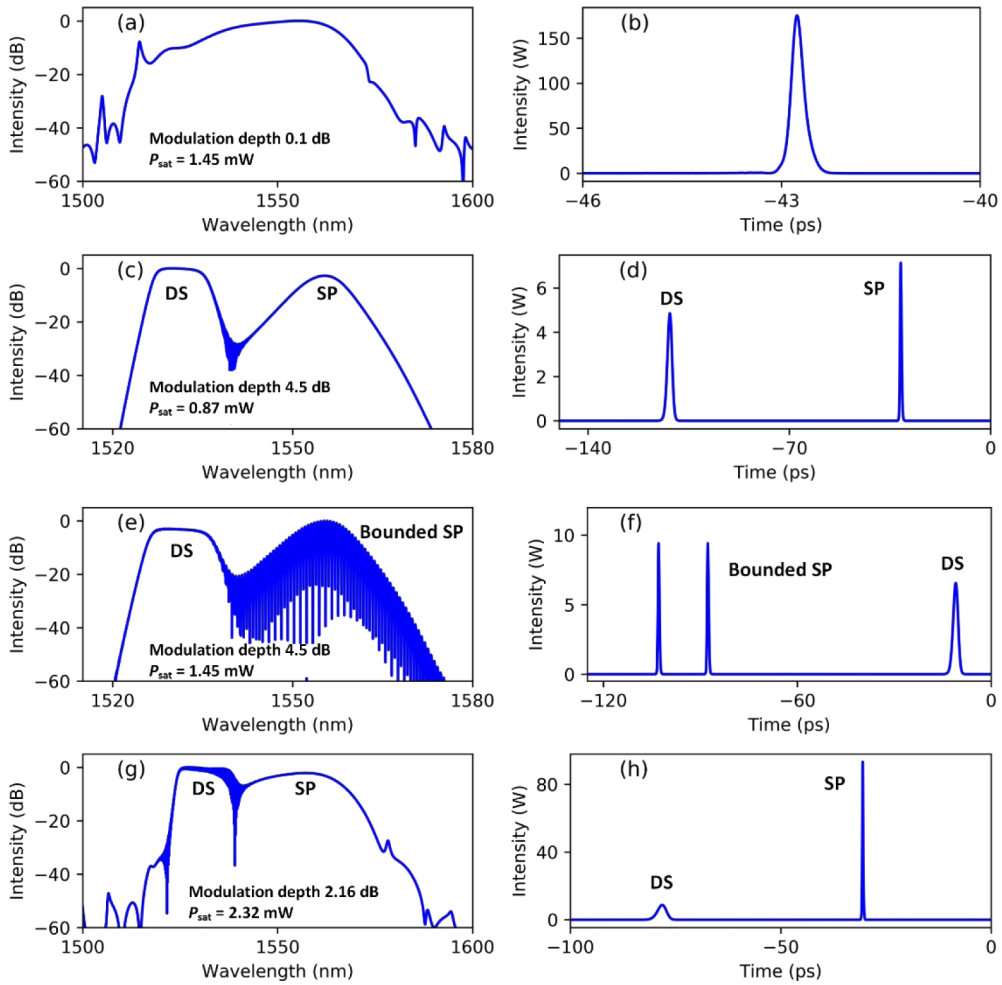

Fig. 4. Simulated results with comb filter: (a) spectrum and (b) waveform with modulation depth of 0.1 dB at P_{sat} of 1.45 mW; (c) spectrum and (d) waveform with modulation depth of 4.5 dB at P_{sat} of 0.87 mW; (e) spectrum and (f) waveform with modulation depth of 4.5 dB at P_{sat} of 1.45 mW; (g) spectrum and (h) waveform with modulation depth of 2.16 dB at P_{sat} of 2.32 mW;

Optics EXPRESS

However, when the P_{sat} scales up to 1.45 mW, the spectrum of the SP shown in Fig. 4(a) exhibits obvious modulation. The corresponding waveform in the time domain splits into two sub-pulses that move together with a fixed distance, indicating a bound-soliton state [37,38]. The FWHM of the DS and bound-SP is 10 nm and 8 nm, respectively. The formation of a dual-wavelength operation opposes to a further broadening of the spectrum with the comb filtering effect. As shown in Fig. 2, the smaller modulation depth results in a broader gain channel. In order to find the widest bandwidth that could be achieved by using a comb filter, we further investigate the smallest modulation depth that required enabling a stable dual-wavelength mode-locking. It is found that the smallest modulation depth is 2.16 dB, and the corresponding widest bandwidth (11 nm for DS and 20 nm for SP) could be obtained at the P_{sat} of 2.32 mW [Fig. 4(g) and 4(h)]. This modulation depth is much larger than the peak-dip difference of the two-peak gain profile, leading to narrower gain channels. Thus, the two-peak gain profile of the EDF are suitable to achieve broadband dual-wavelength pulses compared to a comb filter in our cavity. However, we note that as the two peaks of saddle-like gain profile generally located around 1530 nm and 1555 nm, the comb filter will be more suitable for producing broadband dual-wavelength pulses with specific requirements such as tunable wavelength separation or switchable center wavelength.

4. Experimental results

In our experiment, typical dual-wavelength pulses can be generated with a fine adjustment of the intra-cavity PCs at the pump power of 43 mW. Figure 5(a) shows the dual-wavelength spectrum possessing two center wavelengths with 26 nm separation. The spectrum located at 1530 nm with a FWHM of 11.5 nm has the characteristic steep spectral edges and a flat spectral top, suggesting that it is a DS [39]. The smooth spectrum centered at 1556 nm with a FWHM of 24 nm has no sidebands, a characteristic of SP. Both the DS and SP have the widest FWHM compared to any previously reported dual-wavelength Er-doped fiber lasers. There are two set of pulse trains recorded on the oscilloscope [Fig. 5(b)]. We note that the two pulse trains have different

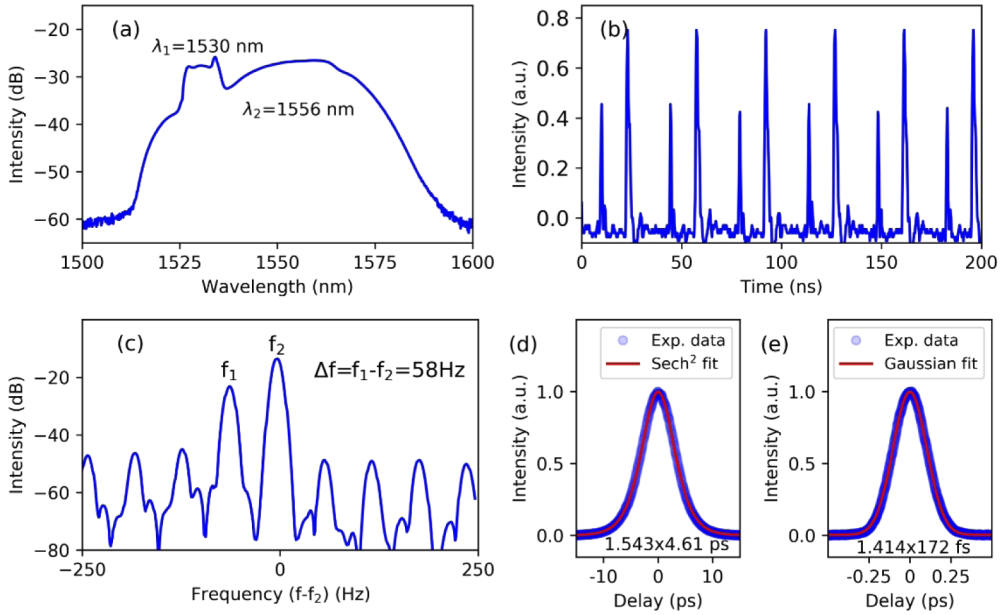

Fig. 5. Experimental results of dual-wavelength operation: (a) spectrum, (b) pulse train, (c) radio frequency (RF) spectrum. The autocorrelation trace of (d) amplified DS at 1530 nm and (e) SP at 1556 nm.

Optics EXPRESS

propagation speed, indicating the existence of asynchronous pulses. The radio frequency (RF) on a span of 500 Hz shows that the dual-wavelength pulses operate at the fundamental frequency of ~28.9036 MHz repetition rates with a difference of 58 Hz [Fig. 5(c)]. The signal to noise ratio (SNR) of the RF spectrum is 52 dB for DS and 61 dB for SP respectively, and the smaller peaks in Fig. 5(c) are beat notes. The SP and DS are then filtered out by a WDM with a passband covering from 1522.5 to 1537.5 nm external to the cavity for autocorrelation trace measurement. The average powers of the SP and DS after WDM are 1.32 mW and 0.52 mW, respectively. Figure 5(d) shows the autocorrelation trace of the DS with a pulse duration of 4.6 ps, fitted with a sech^2 fit. The autocorrelation trace of the SP has a pulse duration of 172 fs with a Gaussian fit [Fig. 5(e)]. We note that the measured average powers and autocorrelation traces of the two pulse trains after the WDM are not precise values as their partially overlapped spectra.

5. Conclusion

In summary, we have proposed a dual-wavelength Er-doped fiber laser mode-locked at near zero dispersion using a BP SA. By exploiting the saddle-like gain profile of EDF and a weak TOD of the fiber, we numerically and experimentally achieve the generation of broad bandwidth SP and DS mode-locking simultaneously. Our proposed compact and simple design provides a new approach for diverse-pattern solitons research and for potential applications such as dual-comb metrology.

Funding

National Natural Science Foundation of China (51778030, 51978024); Engineering and Physical Sciences Research Council (EP/L016087/1).

Disclosures

The authors declared that they have no conflicts of interest to this work.

References

1. X. M. Liu, D. D. Han, Z. P. Sun, C. Zeng, H. Lu, D. Mao, Y. D. Cui, and F. Q. Wang, "Versatile multi-wavelength ultrafast fiber laser mode-locked by carbon nanotubes," Sci. Rep. **3**(1), 2718 (2013).
2. Y. Wei, B. W. Li, X. M. Wei, Y. Yu, and K. K. Y. Wong, "Ultrafast spectral dynamics of dual-color-soliton intracavity collision in a mode-locked fiber laser," Appl. Phys. Lett. **112**(8), 081104 (2018).
3. J. Fellinger, G. Winkler, A. S. Mayer, L. R. Steidle, and O. H. Heckl, "Tunable dual-color operation of Yb:fiber laser via mechanical spectral subdivision," Opt. Express **27**(4), 5478–5486 (2019).
4. H. Zhang, D. Y. Tang, X. Wu, and L. M. Zhao, "Multi-wavelength dissipative soliton operation of an erbium-doped fiber laser," Opt. Express **17**(15), 12692–12697 (2009).
5. S. Mehravar, R. A. Norwood, N. Peyghambarian, and K. Kieu, "Real-time dual-comb spectroscopy with a free-running bidirectionally mode-locked fiber laser," Appl. Phys. Lett. **108**(23), 231104 (2016).
6. J. Chen, X. Zhao, Z. J. Yao, T. Li, Q. Li, S. G. Xie, J. S. Liu, and Z. Zheng, "Dual-comb spectroscopy of methane based on a free-running Erbium-doped fiber laser," Opt. Express **27**(8), 11406–11412 (2019).
7. G. Hu, T. Mizuguchi, X. Zhao, T. Minamikawa, T. Mizuno, Y. Yang, C. Li, M. Bai, Z. Zheng, and T. Yasui, "Measurement of absolute frequency of continuous-wave terahertz radiation in real time using a free-running, dual-wavelength mode-locked, erbium-doped fibre laser," Sci. Rep. **7**(1), 42082 (2017).
8. X. Zhao, Z. Zheng, L. Liu, Q. Wang, H. Chen, and J. Liu, "Fast, long-scan-range pump-probe measurement based on asynchronous sampling using a dual-wavelength mode-locked fiber laser," Opt. Express **20**(23), 25584–25589 (2012).
9. D. Mao, X. Liu, D. Han, and H. Lu, "Compact all-fiber laser delivering conventional and dissipative solitons," Opt. Lett. **38**(16), 3190–3193 (2013).
10. S. Wang, Z. Zhao, and Y. Kobayashi, "Wavelength-spacing controllable, dual-wavelength synchronously mode locked Er:fiber laser oscillator based on dual-branch nonlinear polarization rotation technique," Opt. Express **24**(25), 28228–28238 (2016).
11. K. Y. Lau, M. H. Abu Bakar, F. D. Muhammad, A. A. Latif, M. F. Omar, Z. Yusoff, and M. A. Mahdi, "Dual-wavelength, mode-locked erbium-doped fiber laser employing a graphene/polymethyl-methacrylate saturable absorber," Opt. Express **26**(10), 12790–12800 (2018).
12. B. W. Liu, Y. Y. Lu, Y. Xiang, X. P. Xiao, Q. Z. Sun, D. M. Liu, and P. P. Shum, "Multiplexed ultrafast fiber laser emitting multi-state solitons," Opt. Express **26**(21), 27461–27471 (2018).

Optics EXPRESS

13. X. Zhao, G. Hu, B. Zhao, C. Li, Y. Pan, Y. Liu, T. Yasui, and Z. Zheng, "Picometer-resolution dual-comb spectroscopy with a free-running fiber laser," Opt. Express **24**(19), 21833–21845 (2016).
14. H. S. Shi, Y. J. Song, T. Li, C. Y. Wang, X. Zhao, Z. Zheng, and M. L. Hu, "Timing Jitter of the Dual-Comb Mode-Locked Laser: A Quantum Origin and the Ultimate Effect on High-Speed Time- and Frequency-Domain Metrology," IEEE J. Sel. Top. Quantum Electron. **24**(5), 1–10 (2018).
15. O. G. Okhotnikov and M. Guina, "Stable single- and dual-wavelength fiber laser mode locked and spectrum shaped by a Fabry–Perot saturable absorber," Opt. Lett. **25**(22), 1624–1626 (2000).
16. Y. Wang, J. Li, B. Zhai, Y. Hu, K. Mo, R. Lu, and Y. Liu, "Tunable and switchable dual-wavelength mode-locked Tm3+-doped fiber laser based on a fiber taper," Opt. Express **24**(14), 15299–15306 (2016).
17. H. H. Li, F. M. Hu, C. Li, Y. Tian, C. Q. Huang, J. J. Zhang, and S. Q. Xu, "Generation of switchable multiwavelength solitons with wide wavelength spacing at 2 mu m," Opt. Lett. **44**(10), 2442–2445 (2019).
18. R. M. Li, H. S. Shi, H. C. Tian, Y. P. Li, B. W. Liu, Y. J. Song, and M. L. Hu, "All-polarization-maintaining dual-wavelength mode-locked fiber laser based on Sagnac loop filter," Opt. Express **26**(22), 28302–28311 (2018).
19. X. Luo, T. H. Tuan, T. S. Saini, H. P. T. Nguyen, T. Suzuki, and Y. Ohishi, "Tunable and switchable all-fiber dual-wavelength mode locked laser based on Lyot filtering effect," Opt. Express **27**(10), 14635–14647 (2019).
20. Z. Yan, Y. Tang, B. Sun, T. Liu, X. Li, P. S. Ping, X. Yu, Y. Zhang, and Q. J. Wang, "Switchable multi-wavelength Tm-doped mode-locked fiber laser," Opt. Lett. **40**(9), 1916–1919 (2015).
21. K. Jiang, Z. Wu, S. Fu, J. Song, H. Li, M. Tang, P. Shum, and D. Liu, "Switchable Dual-Wavelength Mode-Locking of Thulium-Doped Fiber Laser Based on SWNTs," IEEE Photonics Technol. Lett. **28**(19), 2019–2022 (2016).
22. Y. S. Fedotov, S. M. Kobtsev, R. N. Arif, A. G. Rozhin, C. Mou, and S. K. Turitsyn, "Spectrum-, pulsewidth-, and wavelength-switchable all-fiber mode-locked Yb laser with fiber based birefringent filter," Opt. Express **20**(16), 17797–17805 (2012).
23. L. Yun, X. Liu, and D. Mao, "Observation of dual-wavelength dissipative solitons in a figure-eight erbium-doped fiber laser," Opt. Express **20**(19), 20992–20997 (2012).
24. H. G. Rosa, D. Steinberg, and E. A. T. de Souza, "Explaining simultaneous dual-band carbon nanotube mode-locking Erbium-doped fiber laser by net gain cross section variation," Opt. Express **22**(23), 28711–28718 (2014).
25. X. Zhao, Z. Zheng, L. Liu, Y. Liu, Y. Jiang, X. Yang, and J. Zhu, "Switchable, dual-wavelength passively mode-locked ultrafast fiber laser based on a single-wall carbon nanotube modelocker and intracavity loss tuning," Opt. Express **19**(2), 1168–1173 (2011).
26. S. Liu, F. P. Yan, L. N. Zhang, Z. Y. Bai, H. Zhou, Y. F. Hou, and N. Zhang, "Switchable SP Dual-Wavelength Mode-Locked TDFL Incorporating a PM-FBG and SESAM," IEEE Photonics Technol. Lett. **29**(6), 551–554 (2017).
27. D. D. Han, X. M. Liu, Y. D. Cui, G. X. Wang, C. Zeng, and L. Yun, "Simultaneous picosecond and femtosecond solitons delivered from a nanotube-mode-locked all-fiber laser," Opt. Lett. **39**(6), 1565–1568 (2014).
28. D. Mao, B. Jiang, W. Zhang, and J. Zhao, "Pulse-State Switchable Fiber Laser Mode-Locked by Carbon Nanotubes," IEEE Photonics Technol. Lett. **27**, 1 (2014).
29. B. Guo, Y. Yao, J. J. Xiao, R. L. Wang, and J. Y. Zhang, "Topological Insulator-Assisted Dual-Wavelength Fiber Laser Delivering Versatile Pulse Patterns," IEEE J. Sel. Top. Quantum Electron. **22**(2), 8–15 (2016).
30. K. X. Li, Y. R. Song, J. R. Tian, H. Y. Guoyu, and R. Q. Xu, "Analysis of Bound-Soliton States in a Dual-Wavelength Mode-Locked Fiber Laser Based on Bi2Se 3," IEEE Photonics J. **9**(3), 1–9 (2017).
31. Y.-Q. Huang, Z.-A. Hu, H. Cui, Z.-C. Luo, A.-P. Luo, and W.-C. Xu, "Coexistence of harmonic soliton molecules and rectangular noise-like pulses in a figure-eight fiber laser," Opt. Lett. **41**(17), 4056–4059 (2016).
32. Y. Z. Wang, J. F. Li, L. J. Hong, G. Y. Li, F. Liu, X. J. Zhou, and Y. Liu, "Coexistence of dissipative soliton and stretched pulse in dual-wavelength mode-locked Tm-doped fiber laser with strong third-order dispersion," Opt. Express **26**(14), 18190–18201 (2018).
33. X. X. Jin, G. H. Hu, M. Zhang, Y. W. Hu, T. Albrow-Owen, R. C. T. Howe, T. C. Wu, Q. Wu, Z. Zheng, and T. Hasan, "102 fs pulse generation from a long-term stable, inkjet-printed black phosphorus-mode-locked fiber laser," Opt. Express **26**(10), 12506–12513 (2018).
34. G. Hu, T. Albrow-Owen, X. Jin, A. Ali, Y. Hu, R. C. T. Howe, K. Shehzad, Z. Yang, X. Zhu, R. I. Woodward, T.-C. Wu, H. Jussila, J.-B. Wu, P. Peng, P.-H. Tan, Z. Sun, E. J. R. Kelleher, M. Zhang, Y. Xu, and T. Hasan, "Black phosphorus ink formulation for inkjet printing of optoelectronics and photonics," Nat. Commun. **8**(1), 278 (2017).
35. D. Mao and H. Lu, "Formation and evolution of passively mode-locked fiber soliton lasers operating in a dual-wavelength regime," J. Opt. Soc. Am. B **29**(10), 2819–2826 (2012).
36. J. Wang, Z. Cai, P. Xu, G. Du, F. Wang, S. Ruan, Z. Sun, and T. Hasan, "Pulse dynamics in carbon nanotube mode-locked fiber lasers near zero cavity dispersion," Opt. Express **23**(8), 9947–9958 (2015).
37. D. Y. Tang, B. Zhao, D. Y. Shen, C. Lu, W. S. Man, and H. Y. Tam, "Bound-soliton fiber laser," Phys. Rev. A **66**(3), 033806 (2002).
38. L. M. Zhao, D. Y. Tang, T. H. Cheng, H. Y. Tam, and C. Lu, "Bound states of dispersion-managed solitons in a fiber laser at near zero dispersion," Appl. Opt. **46**(21), 4768–4773 (2007).
39. W. H. Renninger, A. Chong, and F. W. Wise, "Dissipative solitons in normal-dispersion fiber lasers," Phys. Rev. A **77**(2), 023814 (2008).